Vol. 5 Issue 3, March - 2021, Pages: 29-35

Insights Into A Hole Transfer Mechanism Between Glucose Oxidase And A P-Type Organic Semiconductor

Abdiyev Jurabek Muzaffar o'gli

Physical-Technical Institute Ngo "Physics-Sun", Academy Of Sciences Of Uzbekistan, Tashkent, Uzbekistan
E-mail: fiztexabdiev@gmail.com

Abstract: *This manuscript describes a bioelectrochemical application of a new class of electrochemically generated hole-transporting (p-type) polymeric semiconductors (HTPS), which are based on carbazole core and the oxiran and thiiran reactive groups. Electrode based on transparent layer of indium tin oxide was electrochemically modified with a layer of HTPS and a monolayer of covalently immobilized glucose oxidase (GOx). The HTPS/GOx-based electrode was investigated for an evaluation of direct hole-transfer between the enzyme and electrode at a bio-electrochemically relevant potential via HTPS layer. The broad linear relationship between the peak-current density and glucose concentration from 2 to 15 mM and high stability of ITO/poly-CzS/GOx-electrode was observed. Moreover, it was determined that charge transfer rate constants are reliable for the establishment of advanced electron transfer between enzyme and electrode for the application of this HTPS/GOx-based electrode in long-lived biofuel cells and amperometric biosensors.*

Keywords – Charge transfer, hole-transporting, organic semiconductor, carbazole, glucose biosensor, glucose oxidase.

1. Introduction

Electrochemistry based on the so-called direct charge transfer could be exploited as a model for better understanding of the charge-transfer (CT) mechanisms' in the bio-electrochemical systems (Saboe et al., 2017; Bostick et al., 2017) such as biosensors (Oztekin et al., 2011), biofuel cells (Zhao et al., 2017; Ramanavicius et al., 1999; Koslowski et al., 2012) and eventually in many other bioelectronics-based devices. However, the actual probability of "direct CT" depends significantly on the distance between a redox-active centre and the electrode as well as the nature and/or modification of the electrode surface (Wang, 2008). One of many of such enzymes is glucose oxidase (GOx) (Wilson et al., 1992), which is the most frequently applied in the design of amperometric biosensors as a biological recognition part (Chen et al., 2013) and has a great potential in development of enzymatic biofuel cells (Ramanavicius et al., 2008). On the other hand, direct CT is the main advantage of the third-generation biosensors, which leads to a high selectivity and lower operational potential of the enzymatic electrode. While designing direct CT based electrodes, a high rate of charge transfer between the active site of enzyme and electrode surface is the crucial and most challenging factor. Wittekindt et al. deduced that the aromatic amino acids, such as tyrosine (Tyr) and tryptophan (Trip) are involved in CT of various biological systems (Wittekindt et al., 2009). Later, Winkler and Gray proposed that hole-hopping should protect enzymes from oxidative damage. This CT mechanism prevents the formation of harmful molecular oxidants (Winkler et al., 2015; Gray et al., 2015). Eventually, this hole-transfer mechanism can be applied to establish CT between enzymes and electrodes, which are used in the design of biosensors and biofuel cells. However, according to the best of our knowledge, the hole-transport mechanism has not been realized and proved in above mentioned enzymatic devices so far. On the other hand, hole (p-type) transporting organic semiconductors (for example that based on carbazole derivatives and polymers) have been employed in the organic electronics, such as organic light emitting diodes (OLED) (Bagdziunas et al., 2016; Reig et al., 2017; Bezugly et al., 2018) and solar cells (Sathiyan et al., 2016).

In this research, an investigation of charge (hole) transfer between the enzyme and electrode was performed on electrodes based on indium tin oxide (ITO) electrochemically modified with a hole-transporting (p-type) polymer-semiconductor (HTPS) based on carbazole and covalently immobilized GOx monolayer. Charge transfer rate constants between HTPS and GOx as well as sensitivity to glucose were determined.

2. Experimental section

2.1 Chemicals and materials. The glucose oxidase (GOx) from *Aspergillus niger* with catalytic-activity of 208 U/mg, and glutaraldehyde solution (25 % in water), cystheamine were purchased from Fluka. The *D*-(+)-glucose was obtained from Carl Roth GmbH&Co. ITO coated glass slide with rectangular surface resistivity of 15-25 Ω/□ as electrode and tetrabutylammonium hexafluorophosphate (TBAHFP) as an organic electrolyte were purchased from Sigma-Aldrich. Dichloromethane (DCM) was distilled over CaH_2 and under Ar atmosphere and stored over the 3 Å microsieves. The solution of 0.10 M TBAHFP in the freshly distilled DCM and under Ar atmosphere was used for the polymerization of organic precursors on the ITO electrode. The solution of 0.5 M glucose was prepared in distilled water at least 24 h before use to allow for the mutarotation of *D*-(+)-glucose; to reach

equilibrium between the α- and β-forms. The sodium acetate – acetic acid buffer, pH 4.0, and phosphate-buffered saline solution, pH 7.2, with 0.55 M of NaCl (1X-PBS) were used in the biosensors investigations.
Precursors of organic polymers as semiconductors (OS) were prepared according to the following literature the 9-(oxiran-2-ylmethyl)-9*H*-carbazole (CzO) (Humphries et al., 2016) and 9-(thiiran-2-ylmethyl)-9*H*-carbazole (CzS) (Swinarew et al., 2011).

2.2 Instrumentation

The electrochemical modification of graphitic electrodes and the amperometric-measurements by cyclic voltammetry (CV) were performed using an Autolab PGSTAT 30 Potentiostat/Galvanostat from Autolab (Utrecht, The Netherlands) that was operated by the Nova 1.10 software. The ITO electrode with the electrochemically active area of 0.65 cm^2 and titan plate electrode (partially coated with platinum) with the electrochemically active-area of 1.0 cm^2 were used as the working- and the counter-electrodes, respectively. An Ag/AgCl-electrode in saturated KCl ($Ag/AgCl/KCl_{sat}$) was used as a reference-electrode in the aqueous-media. Ag wire was used as the reference, and graphitic electrode – as the counter-electrode in the non-aqueous-media, respectively. In this case, ferocene/ferocenium couple was employed as the external reference red-ox system. Attenuated total reflection infrared (ATR IR) spectra were recorded using a Bruker VERTEX 70 spectrometer. The static contact angle was measured using a Theta Lite optical tensiometer and contact angle meter from Biolin Scientific. The atomic force microscopy (AFM) was carried out using a WITec Alpha300R microscope.

2.3 Electrochemical modification and investigation of electrode by the organic semiconductors based layers

Before the modification of ITO-modified glass electrode, the electrodes were washed with distilled water and acetone; afterwards they were electrochemically cleaned by 10 potential cycles in the range from -1000 to +1000 mV *vs* $Ag/AgCl/KCl_{sat}$, at 200 mV/s scan rate in BPS buffer solution. The cleaned ITO electrodes were electrochemically modified by 10 potential cycles in solution of 0.5 mg/ml of the CzO and CzS organic precursors in 0.1 M TBAHFP dissolved in dry DCM at the scan rate of 50 mV/s. During this modification (the potential was swept from -200 mV to +1500 mV *vs* Ag/AgCl for polymerization of CzO and CzS) cyclic voltammograms were registered. In order to clean formed ITO/*poly*-CzO- and ITO/*poly*-CzS - electrodes they were washed with distilled water before and after each treatment step. An electrochemical characterization was performed with the same electrochemical devices and software which were used for the modification of ITO electrodes.

2.4 Immobilization of GOx on ITO/*poly*-CzO and ITO/*poly*-CzS -electrode

After electrochemical modification of the ITO/*poly*-CzO-, ITO/*poly*-CzS electrodes and clean ITO for reference, first of all, they were being incubated in the cysteamine solution in distilled water (80 mg mL^{-1}, 1 M) for one hour at a room temperature. Afterwards, the electrodes were being incubated for 1 hour at room temperature in a solution 2.5% of glutaraldehyde in water. The electrodes were washed with distilled water before and after each treatment step. Finally, the following electrodes were immersed to a GOx (5 mg/mL) solution in PBS buffer (pH 7.2) and stored for 24 hours at +4^{o}C temperature. Prior to the electrochemical measurements, the electrodes were thoroughly washed with distilled water in order to remove: the non-immobilised enzyme; the dissociated GOx cofactor – FAD; and the other un/non-immobilized materials, which were present in the enzyme samples used for electrode modification. Moreover, an immobilization of the pure FAD cofactor on the ITO/*poly*-CzS -electrode was not observed using the UV-vis spectroscopy due to a low nucleophilicity of the amino group of the FAD cofactor adenine. The prepared electrodes had been kept in a closed-vessel over PBS, pH 7.2, at +4^{o}C until they were used in the experiments.

3. Results and discussion.

3.1 Electrode modification and properties. For the synthesis of electroactive polymer, the 9-(oxiran-2-ylmethyl)-9*H*-carbazole (CzO) and 9-(thiiran-2-ylmethyl)-9*H*-carbazole (CzS) derivatives were employed as electro-polymerizable organic semiconductor monomers. It is universally accepted that during electrochemical oxidation carbazole derivatives mostly couple to each other *via* 3- and 6-position (Fig. 1, a) due to the fact that these molecules have the highest electron densities at these positions (Karon et al., 2015). The electrochemical deposition of polymers *poly*-CzO and *poly*-CzS on ITO surface was performed under the potentiodynamic conditions (Fig. 1a and b). The onset ionisation potentials (IP) of monomer and polymer were measured during the 1st and 10th potential cycles of electrochemical-polymerization, respectively. The ionization potentials were calculated to be 1.15/1.12 V *vs* Ag/AgCl (5.61/5.58 eV *vs* vacuum) and 0.882/0.773 V (5.34/5.24 eV) for CzO/CzS monomers and *poly*-CzO/*poly*-CzS polymers, respectively. Furthermore, *poly*-CzS is obtained at a lower ionization potential than *poly*-CzO due to the longer polymer chains and their higher conjugations.

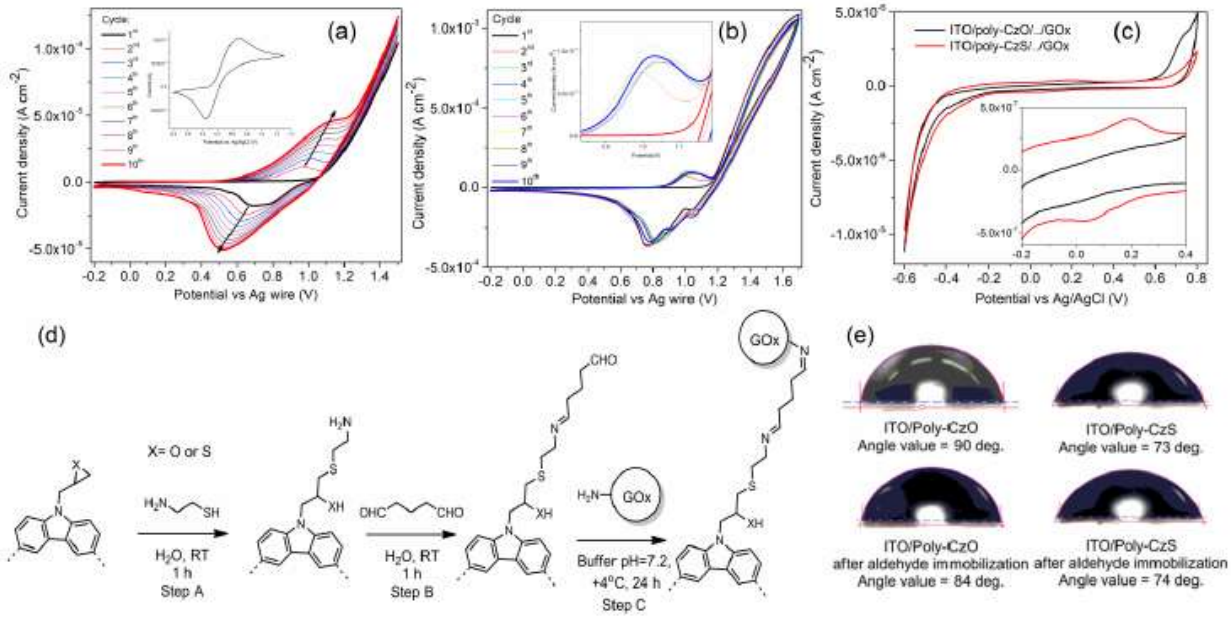

Figure 1. Electrode modification and evaluation. Cyclic voltammogram (CV) profiles of ITO-electrode during potential cycling based electrochemical polymerization of (**a**) CzS and (**b**) CzO in DCM 0.1 M of $NaBu_4PF_6$ at scan rate of 50 mV s^{-1},1st to 10th cycle (Inset: CV of ferrocene as external standard), (**c**) CVs of ITO/*poly*-CzO and *poly*-CzS/amine/aldehyde/GOx in buffer, pH 4.0, (Inset: increased spectral range from -0.2 to 0.4 V), (**d**) schematic representation of step-by-step self-assembly-based immobilization of GOx on ITO/*poly*-CzO and ITO/*poly*-CzS electrodes, (**e**) water contact angle measurements of ITO/*poly*-CzO(S) electrode before and after the treatment with glutaraldehyde.

During the verification of the polymer's chemical structure, both monomer and polymer films on ITO were analysed using attenuated total reflection infrared (ATR IR) spectroscopy. The bending vibrations situated at 747 cm^{-1} and 749 cm^{-1} for CzO and CzS, respectively, corresponded to the vibration of carbazyl core. Moreover, the formation of polymeric carbazyl in electrochemical deposition film was approved by IR spectra in accordance with the appearance of the new peaks at 826 cm^{-1} and 832 cm^{-1}, which indicated the formation of trisubstituted carbazole moieties (Liu et al., 2015). Furthermore, the stability of oxirane and thiirane groups during electrochemical deposition was evaluated by IR. In the spectrum of CzO, medium-intensive C-O bond vibration signals of oxirane group were observed at 861 cm^{-1} and 908 cm^{-1}, which correspond to scissoring and symmetric stretching of the oxirane cycle (Fig. 2a). After electrochemical polymerization, the peak in *poly*-CzO spectra shifted to the 883 cm^{-1} (Nikolic et al., 2010). For CzS, a band at about 598 cm^{-1} could be attributed to C-S bond vibrations in thiirane group (Allen et al., 1986). The corresponding band in the spectrum of *poly*-CzS film at 560 cm^{-1} was indicated (Fig. 2b). The results indicate that the successful generation of the polycarbazole films has been achieved by the polymerisation of the CzO and CzS precursors.

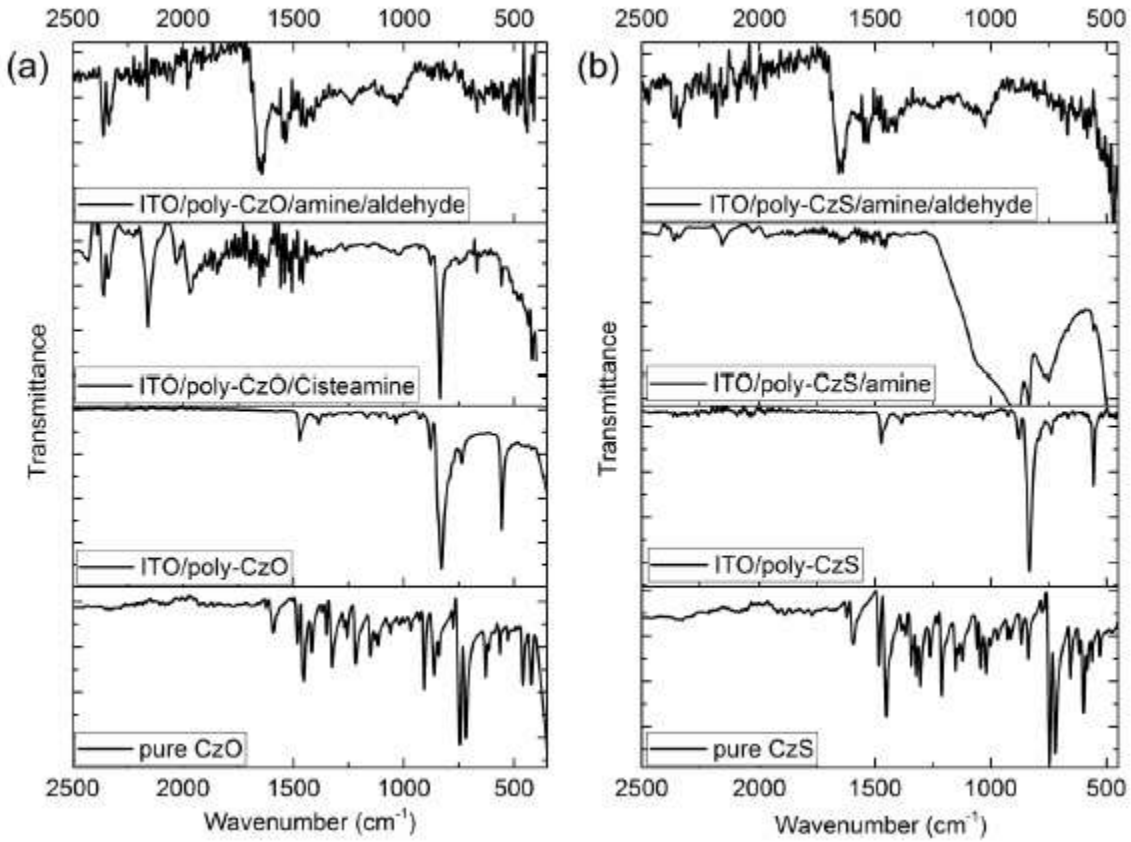

Figure 2. ATR-IR spectra of (**a**) pure CzO and (**b**) pure CzS, both deposited on ITO/*poly*-CzO(S), ITO/*poly*-CzO(S)/amine, ITO/*poly*-CzO(S)/amine/aldehyde.

A step-by-step covalent-binding-based assembly was applied for the immobilization of GOx (Samanta et al., 2011). First of all, the electrodes with polycarbazole films were incubated in the aqueous cysteamine solution. At this stage, monolayer containing the amine groups was formed (Fig. 1d, Step A). Secondly, the free terminal amine groups were functionalized with glutaraldehyde in water (step B) *via* the aldehyde and amine condensation reaction to imine at a room temperature. From IR spectra of both ITO/CzS(O)/amine/aldehyde surfaces, the signal of aldehyde C=O group vibration at 1730 cm^{-1} was observed (Fig. 2a,b). Finally, ITO/CzS(O)/amine/aldehyde electrodes were incubated in GOx (5 mg mL^{-1}) solution in buffer, pH 7.2, and stored for 24 hours at +4 ^{o}C temperature. It should be noted that the immobilization of GOx directly on the *poly*-CzO and *poly*-CzS surfaces does not occur because these surfaces are hydrophobic (evaluated below) and the oxiran(or thiiran)-2-ylmethyl tags are too short (only 4 Å) for imine formation reaction. Moreover, water solvation shell, which is formed around the hydrophobic side chains on the enzyme surface that is in the range of ~10 Å, prevents the reaction with too short tags (Fogarty et al., 2014). ITO/*poly*-CzS surface is more hydrophilic in comparison to that of ITO/*poly*-CzO. However, small differences of surface roughness between the immobilized and pure polymer surfaces were observed by AFM imaging (Fig. 3). It should be noted that the surface wettability is significantly influenced by surface roughness (Marmur, 2006).

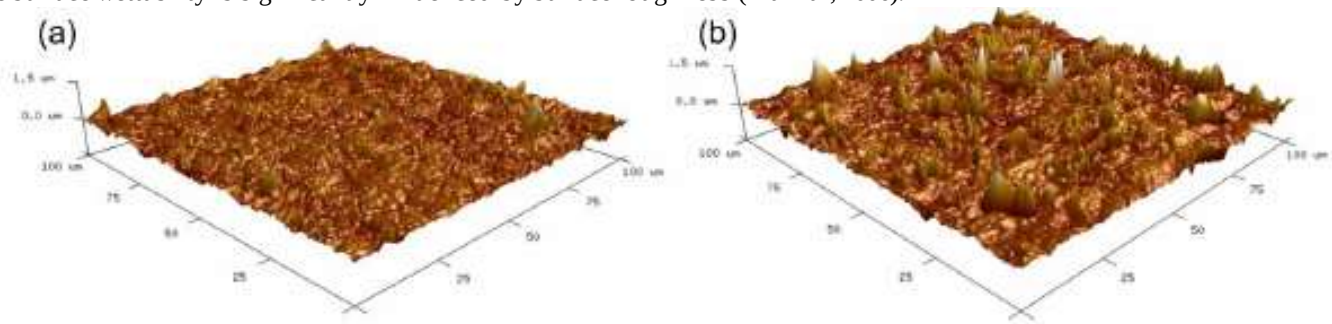

Figure 3. AFM images of (**a**) ITO/*poly*-CzS and (**b**) the same surface after GOx immobilization.

3.2 Electrochemical evaluation of modified electrodes

The electrochemical experiments were carried out to verify the mechanism and efficiency of charge transfer (CT) between the GOx-cofactor and semiconducting *poly*-CzS or *poly*-CzO layers, surface-activity, and the diffusion rate coefficient. However, the CT from GOx only in ITO/*poly*-CzS/GOx-based electrode was observed (Fig. 1c) due to a higher conductivity and lower ionization potential (5.58 eV *vs.* 5.24 eV) of *poly*-CzS. CVs illustrated that CT in ITO/*poly*-CzS/GOx-based electrode is quasi-reversible and surface-controlled. Moreover, any new signals in the CVs and FT-IR spectra were observed in the bare ITO electrode after the immobilization. Efficiency of charge (either electrons or holes) transfer was estimated from the peak shape of CV. It is diagnostic of the homogeneity of the mono-layer and can be evaluated by the full width at half of the peak full width at half maximum (FWHM) as described by equation *1*:

$$n = \frac{3.53\ RT}{FWHM \times F} = \frac{90.6\ mV}{FWHM} \quad (1)$$

where *n* is the number of charge carriers (electrons or holes), *R* is an ideal gas constant, *T* is an absolute temperature and *F* is a Faraday constant.

The values of FWHM can be larger or smaller than theoretical FWHM have been attributed to electrostatic effects incurred by the neighbouring charged species (Bard et al., 2001). According to the electrochemical measurements, a quasi-reversible surface-controlled electrochemical process was observed and the full width at half of the peaks maximum heights (FWHM) were calculated to be 115 and 120 mV for the positive and negative signals of the ITO/*poly*-CzS/GOx system, respectively, which satisfies the one electron (or one hole) based charge transfer process. Moreover, the oxidation peaks at pH 4.0 and 7.2 registered at scan rate of 10 mV s^{-1} was observed at 181 mV and 76 mV *vs* Ag/AgCl (4.82 eV and 4.71 eV), what corresponds to the reversible/monoelectronic oxidation of $FADH_2$ to $FADH_2^+$. To evaluate the reversible charge transfer phenomenon in more detail, CVs at different scan rates at pH 4.0 and 7.2 were recorded (Fig. 4).

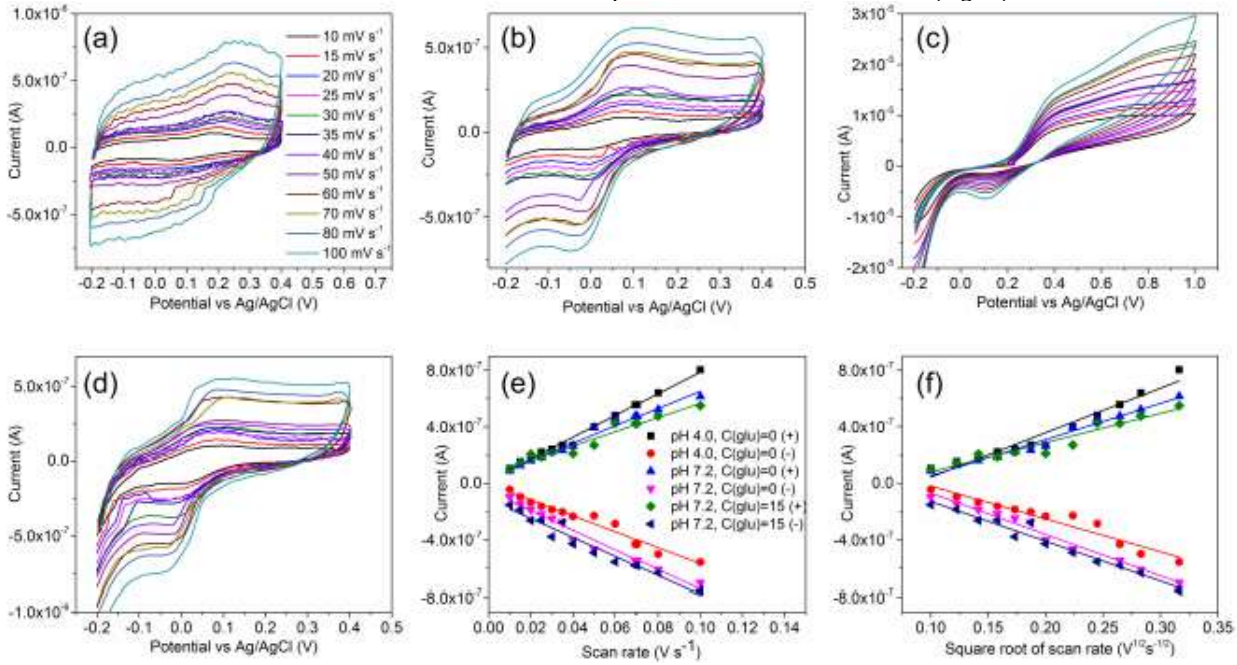

Figure 4. (**a**) CVs at different scan rates when pH 4.0 and C(glu)=0, (**b**) pH 7.2 and c(glu)=0, (**c**), pH 4.0 and c(glu)=15 mM, (**d**) pH 7.2 and C(glu)=15 mM, (**d**) current *vs* scan rate and (**f**) current *vs* square root of scan rate and the corresponding fitting lines. Scan rates in the range from 10 to 100 mV s^{-1} were used for all CV experiments.

The surface activity *Γ* (coverage), which in this particular system is the activity of the GOx immobilized on particular area of electrode-surface, and it was determined from the slope of the line of *I vs v*, using equation *2*:

$$\Gamma = \frac{4IRT}{n^2F^2A}v \quad (2)$$

where *I* is a peak current, *v* is potential sweep rate, *A* is area of the electrode. Activity of ITO/*poly*-CzS/GOx-surface at pH 4.0 and 7.2 without glucose were calculated from the slope of the linear oxidation current dependence *vs* sweep rate to be about 3 10^{-12} mol cm^{-2}. For the calculation of theoretical surface-coverage, a diameter of GOx monomer of 65 Å and a filling 12 ratio of 0.8 were proposed. Then the theoretical surface-concentration of the GOx molecules on the surface of electrode (coverage of electrode

by GOx) was calculated to be 4×10^{-12} mol cm^{-2}. This value is in-line with experimental Γ value. Very similar activity of ITO/*poly*-CzS/GOx-electrode was observed after one month storage at +4 ^{o}C in the buffer solution. Therefore, we think that the hole-hopping-based charge-transfer from GOx to organic semiconductor protected the enzyme from oxidative damage.

The pH influence on the rate-constants of ITO/*poly*-CzS/GOx structure at pH 4.0 and 7.2 was investigated and compared. First of all, the surface-activities for oxidation and reduction at pH 7.2 and 4.0 are very similar, i.e., about 3 10^{-12} mol cm^{-2}. Secondly, considering the influence of glucose on the charge transfer, ITO/*poly*-CzS/GOx-electrode at pH 4.0 and 7.2 was investigated employing a relatively high glucose concentration of 15 mM. The oxidation and reduction rate constants at pH 7.2 were estimated as being statistically of the same value with that one registered in a similar system without glucose (Table 1, entry 3 and 4) because this is a charge (hole) transfer process from the HTPS to the cofactor. However, for a system with glucose at pH 4.0, a new irreversible peak at about 800 mV was observed (Fig. 4c). The first signal at about 180 mV (onset) exhibits oxidation of the cofactor to the radical cation *via* holes from the organic semiconductor. The second signal at about 800 mV can be assigned to the oxidation of the FAD-glucose complex to gluconic acid and FAD (see below). According to (Tao et al. 2009), the second order rate constant of glucose oxidation in the presence of GOx is about 3×10^{4} M^{-1} s^{-1}. Therefore, the pseudo-first order rate constant at 15 mM of glucose of this process was calculated to be 450 s^{-1}. The lower k_{CT} of reduction process at pH 4.0 than oxidation of glucose suggests that glucose can moderate the CT kinetics in the enzyme. Recently, Bartlett and Al-Lolage (Bartlett and Al-Lolage, 2017) have analyzed the scientific papers, which reported electrochemical biosensors based on glucose oxidase (GOx), that were purified by different suppliers from different GOx-producing microorganisms. They have predicted that the redox peaks in cyclic voltammograms, which are usually attributed to charge transfer of GOx sometimes arise from free FAD, and possibly from catalase and/or other impurities, which are present in the as supplied commercial enzyme that are also adsorbed at the electrode's surface. It was reported, that in the case of immobilized catalase, a more negative obvious catalytic reduction peak is observed (Salimi, et al., 2005) when compared to that observed in our recent research. Free FAD has been washed out by a tough washing procedure of GOx-modified electrodes. Moreover, the possibility that some free FAD cofactor is released from the slowly dissociating GOx and can be oxidized/reduced on the electrode's surface cannot be excluded, because the cofactor – FAD – binds with apo-GOx non-covalently, therefore this binding is relatively weak and holo-GOx tends to dissociate slowly into apo-GOx and FAD.

3.3 Dependence of electrode current on glucose concentration in solution

If biofuel cells are implanted within patient's body, they should operate within actual range of glucose biosensors, which is in the range of 4-8 mM. Volt-amperometric behaviour of ITO/*poly*-CzS/GOx-electrode was investigated by cyclic voltammetry in potential range from -200 mV until +1000 mV in the presence of different glucose concentrations (1-15 mM) in buffer, pH 4.0, and containing dissolved oxygen (Fig. 5a). After addition of glucose, the difference of current for the oxidation (at 800 mV) peaks was calculated. A broad linear relationship of the peak-current density and glucose concentration from 2 to 15 mM was observed (Fig. 5a, inset); with correlation coefficient of 0.982 for the oxidation currents. Moreover, from the slope of linear fitting, the sensitivity to glucose is estimated to be 0.64±0.03 μA mM^{-1} cm^{-2}. According to (Su et al, 1999), the second-order rate constant for oxidation of $FADH_2$ in GOx by oxygen at low pH was estimated to be 1.6 10^{6} M^{-1} s^{-1}. Therefore, the pseudo-first order oxidation rate constant at ~0.2 mM of O_2 dissolved in water was calculated to be ~300 s^{-1}.

Based on the obtained results, the mechanism of glucose oxidation *via* holes and without involvement of dissolved oxygen was proposed (Fig. 5b). First of all, holes from the electrode in reversible way oxidise the $FADH_2$ cofactor into radical cation – $FADH_2^{+}$. Therefore, the oxidation and reduction peaks are observed in the CV at around +400 mV and +100 mV, respectively (Fig. 5a). A second step is a nucleophilic addition of glucose to this radical cation ($FADH_2^{+}$) and the formation of transition state (TS). Recently, similar TS of the FAD-glucose complex has been successfully identified using a mass spectrometry (Wang, et al., 2017). Finally, the formed TS is oxidized by second hole from the electrode to form initial $FADH_2$ and gluconic acid.

4. Conclusions and future trends

In this study, a class of hole-transferring (p-type) organic/polymeric semiconductor, which is acting as a redox polymer, based on the carbazole core and oxiran and thiiran reactive groups is applied in the biosensor electrode design. These compounds were electrochemically polymerized and deposited on the ITO electrode surface as the electroactive-layer. Then step-by-step covalent-binding-based assembly was applied for the immobilization of glucose oxidase monolayer. The electrochemical experiments showed a direct hole-transfer from the electrode towards enzyme at relatively low ionisation potential. The charge-transfer rate-constants for oxidation and reduction of flavin adenine dinucleotide cofactor are about 130 s^{-1} and 160 s^{-1}, respectively. Moreover, the broad linear relationship between the peak-current density and glucose concentration from 2 to 15 mM and high stability of ITO/*poly*-CzS/GOx-electrode has been observed. These experimental findings contribute to the development and investigation of new hole-transferring materials suitable for application in the design of biofuel cells, electrochemical biosensors and other bioelectronics-based devices.

Advanced calculations of charge transfer between hole-transferring (p-type) organic/polymeric semiconductors and GOx will be published elsewhere, this new research will be based on theoretical methods such as the Marcus theory and the density functional theory (DFT) and it will be supported by additional insights and interpretations.

5. References

Allen, W.D., Bertie, J.E., Falk, M.V., Hess, B.A., Mast, G.B., Othen, D.A., Schaad, L.J., Schaefer, H.F., 1986. J. Chem. Phys. 84 (8), 4211–4227.

Bagdžiūnas, G., Grybauskaitė, G., Kostiv, N., Ivaniuk, K., Volyniuk, D., Lazauskas, A., 2016.
RSC Adv. 6 (66), 61544–61554.

Bard, A.J., Faulkner, R.L., 2001. Electrochemical Methods: Fundamentals and Applications, 2nd ed., John Wiley & Sons, Inc., New York.

Bartlett, P.N., Al-Lolage, F.A., 2017. J. Electroanal. Chem. doi:10.1016/j.jelechem.2017.06.021 Bezuglyi, M., Ivaniuk, K., Volyniuk, D., Gražulevičius, J.V., Bagdžiūnas, G., 2018. Dyes and Pigments 149, 298–305.

Bostick, C.D., Mukhopadhyay, S., Pecht, I., Sheves, M., Cahen, D., Lederman, D., 2017. Protein Bioelectronics: A Review of What We Do and Do Not Know. arXiv:1702.05028.

Chen, C., Xie, Q., Yang, D., Xiao, H., Fu, Y., Tan, Y., Yao, S., 2013. RSC Adv. 3 (14), 4473– 4491.

Demin, S., Hall, E.A.H., 2009. Bioelectrochemistry. 76 (1), 19–27.

Deng, C., Chen, J., Chen, X., Xiao, C., Nie, L., Yao, S., 2008. Direct Electrochemistry of Glucose Oxidase and Biosensing for Glucose Based on Boron-Doped Carbon Nanotubes Modified Electrode. Biosens. Bioelectron. 23 (8), 1272–1277.

Fogarty, A.C., Laage, D., 2014. J. Phys. Chem. B. 118 (28), 7715–7729.

Gray, H.B., Winkler, J.R., 2015. PNAS. 112 (35), 10920–10925.

Humphries, P.S., Bersot, R., Kincaid, J., Mabery, E., McCluskie, K., Park, T., Renner, T., Riegler, E., Steinfeld, T., Turtle, E.D., Wei, Z.-L., Willis, E., 2016. Bioorg Med Chem Lett. 26 (3), 757–760.

Karon, K., Lapkowski, M., 2015. J Solid State Electrochem. 19 (9), 2601–2610.

Koslowski, T., Burggraf, F., Krapf, S., Steinbrecher, T., Wittekindt, C., 2012. Biochim. Biophys.
Acta. 1817 (10), 1955–1957.

Liu, C., Luo, H., Shi, G., Yang, J., Chi, Z., Ma, Y., 2015. J. Mater. Chem. C. 3 (15), 3752–3759.

Liu, J., Paddon-Row, M.N., Gooding, J.J., 2006. Chemical Physics. 324 (1), 226–235.

Marmur, A., 2006. Soft Matter. 2 (1), 12–17.

Nikolic, G., Zlatkovic, S., Cakic, M., Cakic, S., Lacnjevac, C., Rajic, Z., 2010. Sensors. 10 (1), 684–696.

Oztekin, Y., Ramanaviciene, A., Yazicigil, Z., Solak, A.O., Ramanavicius, A., 2011. Biosens.
Bioelectron. 26 (5), 2541–2546.

Ramanavicius, A., Habermüller, K., Csöregi, E., Laurinavicius, V., Schuhmann, W., 1999. Anal.
Chem. 71 (16), 3581–3586.

Ramanavicius, A., Kausaite, A., Ramanaviciene, A., 2008. Biosens. Bioelectron. 24 (4), 761– 766.

Reig, M., Gozálvez, C., Bujaldón, R., Bagdziunas, G., Ivaniuk, K., Kostiv, N., Volyniuk, D., Grazulevicius, J.V., Velasco, D., 2017. Dyes and Pigments. 137, 24–35.

Saboe, P.O., Conte, E., Farell, M., Bazan, G.C., Kumar, M., 2017. Energy Environ. Sci. 10 (1), 14–42.

Salimi, A., Noorbakhsh, A., Ghadermarz, M., 2005. Anal. Biochem. 344, 16–24. doi:10.1016/j.ab.2005.05.035

Samanta, D., Sarkar, A., 2011. Chem. Soc. Rev. 40 (5), 2567–2592.

Sathiyan, G., Sivakumar, E.K.T., Ganesamoorthy, R., Thangamuthu, R., Sakthivel, P., 2016.
Tetrahedron Lett. 57 (3), 243–252.

Su, Q., Klinman, J.P., 1999. Biochemistry 38, 8572–8581.

Swinarew, A., Stolarzewicz, A., Grobelny, Z., Swinarew, B., Grazulevicius, J.V., Simokaitiene, J., Andrikaityte, E., 2011. J. Mol. Struct. 1005 (1), 129–133.

Tao, Z., Raffel, R.A., Souid, A.-K., Goodisman, J., 2009. Biophys. J. 96 (7), 2977–2988.

Wang, J., 2008. Chem. Rev. 108 (2), 814–825.

Wang, Y., Sun, M., Qiao, J., Ouyang, J., Na, N., 2017. Chem. Sci. doi:10.1039/C7SC04259K Wen, Z., Ye, B., Zhou, X.,
1997. Electroanalysis. 9 (8), 641–644. Wilson, R., Turner, A.P.F., 1992. Biosens. Bioelectron. 7 (3), 165–185.

Willner, I., Heleg-Shabtai, V., Blonder, R., Katz, E., Tao, G., Bückmann, A.F., Heller, A., 1996.
J. Am. Chem. Soc. 118, 10321–10322.

Winkler, J.R., Gray, H.B., 2015. Q Rev Biophys. 48 (4), 411–420.

Wittekindt, C., Schwarz, M., Friedrich, T., Koslowski, T., 2009. J. Am. Chem. Soc. 131 (23), 8134–8140.

Wohlfahrt, G., Witt, S., Hendle, J., Schomburg, D., Kalisz, H.M., Hecht, H.-J., 1999. Acta Cryst D. 55 (5), 969–977.

Zhao, C., Gai, P., Song, R., Chen, Y., Zhang, J., Zhu, J.-J., 2017. Chem. Soc. Rev. 46 (5), 1545– 1564